

## Effects of depth- and CO<sub>2</sub>-dependent C:N ratios of particulate organic matter (POM) on the marine carbon cycle

Birgit Schneider,<sup>1</sup> Anja Engel, and Reiner Schlitzer

Alfred Wegener Institut für Polar- und Meeresforschung, Bremerhaven, Germany

Received 10 November 2003; revised 12 March 2004; accepted 7 April 2004; published 5 June 2004.

[1] According to a recent study, C:N ratios of sinking particulate organic matter (POM) in the ocean appear to be higher than Redfield (7.1 instead of 6.6) and depth dependent (increase +0.2/km). Here we investigate the effects of vertically variable C:N element ratios on marine carbon fluxes and the air-sea exchange of CO<sub>2</sub> using a global ocean carbon cycle model (AAMOCC). For a steady-state ocean, the results show that models using the constant classical Redfield ratio underestimate both, total inventory and vertical gradients of dissolved inorganic carbon (DIC). While the amount of additional DIC (+150 Gt C) is negligible compared to the high marine carbon inventory, the C:N depth dependence can reduce the ambient atmospheric pCO<sub>2</sub> by 20 ppm, permanently. Moreover, the simulation of a future scenario, estimating a possible effect of CO<sub>2</sub>-dependent C:N ratios of POM on the marine carbon cycle, has shown that even a moderate rise in the C:N element ratio of sinking POM, which is on the order of magnitude of natural variability, yields a considerably higher oceanic uptake of anthropogenic CO<sub>2</sub> on timescales of decades to centuries. The assumption is based on a predicted increase in the production of highly carbon enriched transparent exopolymer particles (TEP) caused by rising atmospheric CO<sub>2</sub> concentrations and enhanced nutrient limitation. However, counteracting a predicted decrease of the physical (solubility) CO<sub>2</sub> pump as a consequence of global change, the effect in our scenario will alleviate further rising atmospheric CO<sub>2</sub> concentrations rather than compensate a reduced physical uptake.

**INDEX TERMS:** 4805 Oceanography: Biological and Chemical: Biogeochemical cycles (1615); 4806 Oceanography: Biological and Chemical: Carbon cycling; 4842 Oceanography: Biological and Chemical: Modeling; 4845 Oceanography: Biological and Chemical: Nutrients and nutrient cycling; **KEYWORDS:** elemental composition of POM, marine particle fluxes, Redfield ratio

**Citation:** Schneider, B., A. Engel, and R. Schlitzer (2004), Effects of depth- and CO<sub>2</sub>-dependent C:N ratios of particulate organic matter (POM) on the marine carbon cycle, *Global Biogeochem. Cycles*, 18, GB2015, doi:10.1029/2003GB002184.

### 1. Introduction

[2] In the surface ocean, biological production transforms dissolved inorganic carbon (DIC) and nutritional elements, such as phosphorus and nitrogen into particulate and dissolved organic matter (POM, DOM). Export of organic matter to the deep ocean is mediated by sinking of large particles and subduction of DOM via deep water formation. The resulting loss of DIC in the surface water is partly replaced by upwelling of DIC enriched deep waters and by exchange with atmospheric CO<sub>2</sub>. These two mechanisms, export of organic matter (biological pump) and the dissolution of CO<sub>2</sub> in the surface water and its downward transport by deep water formation (physical pump), are the main processes leading to an exchange of CO<sub>2</sub> between ocean and atmosphere [Volk and Hoffert, 1985]. A quanti-

tative understanding of the oceans uptake and storage capacity for CO<sub>2</sub> is essential to reliably predict the future concentration of CO<sub>2</sub> in the atmosphere and consequences for climate changes.

[3] In order to assess the biological sequestration of CO<sub>2</sub> by the ocean, biogeochemical models often relate carbon to nitrogen and phosphorus fluxes assuming Redfield stoichiometry [Redfield *et al.*, 1963]. Following this concept the biological carbon cycling in the ocean is directly related to nitrogen and phosphorus turnover by a molar ratio of 106:16:1:–138 (C:N:P:O). Although this concept strongly simplifies the calculation of biogeochemical cycles, it otherwise sets a theoretical limit for the sequestration of organic carbon to the deep sea. Moreover, it has been observed that some oceanic regions can exhibit strong non-Redfieldian behavior in the consumption of DIC and nutrients [Michaels *et al.*, 1994; Arrigo *et al.*, 1999; Körtzinger *et al.*, 2001]. This observation is in accordance with biological process studies, showing that carbon uptake can be temporarily decoupled from nitrogen and phosphorus [Banse, 1974; Engel *et al.*, 2002] and with the analysis of a

<sup>1</sup>Now at Institut für Geowissenschaften, Kiel, Germany.

**Table 1.** Parameters for Atmospheric pCO<sub>2</sub>, C:N Ratios of POM at the Base of the Euphotic Zone ( $z_{EZ}$ ), C:N Depth Dependence, Simulated Time Interval, and the Initial Tracer Fields for the Experiments (I–IV) Carried Out in This Study

Experiment	Atmosphere	C:N Ratio at $z_{EZ}$	C:N Depth Dependence	Simulated Time	Source of Initial Tracer Field
I	278 ppm	6.6	no	5000 years	optimization
II	278 ppm	7.1	yes	8000 years	I
III	S650	7.1	yes	1770–2200	II
IV	S650	7.1–8.1	yes	1770–2200	II

global data set of C:N ratios from material caught in sediment traps [Schneider *et al.*, 2003]. The latter study revealed that the average molar C:N ratio of sinking particles in the surface water is significantly higher than the classical Redfield ratio (RR) ( $7.1 \pm 0.1$  instead of 6.6) and increases over depth by  $0.2 \pm 0.1$  units per 1000 m water depth. As many model studies extrapolate the oceanic carbon export from the availability of nitrogen and/or phosphorus in the surface water by prescribing Redfield stoichiometry, a possible decoupling of carbon and nitrogen cycles is not considered. Consequently, these models may either underestimate carbon fluxes or overestimate nitrogen fluxes.

[4] The aim of the current study is to determine the effects of spatial (vertical) and temporal (decadal to centennial) variations in the C:N elemental composition of POM on the marine carbon cycle, using a global coupled physical-biogeochemical ocean carbon cycle model (AAMOCC). First, two equilibrated global ocean systems are compared, one of them with particle fluxes according to the constant classical RR, while the other one simulates particle compositions complying with results of Schneider *et al.* [2003]. Starting from the second equilibrium state, two time-dependent (preindustrial to future) simulations are carried out with prescribed atmospheric pCO<sub>2</sub> variation. Doing so, in one experiment, particle compositions are kept temporally constant, whereas the second time-dependent simulation provides a possible scenario for a CO<sub>2</sub> sensitivity of POM-element ratios, which are now coupled to the atmospheric pCO<sub>2</sub> development.

## 2. Model

### 2.1. AAMOCC

[5] The model applied in this study is the AWI Adjoint Model for Oceanic Carbon Cycling (AAMOCC) [Schlitzer, 2000, 2002, 2004]. It is a 3-D ocean circulation model simulating global distributions of dissolved inorganic carbon (DIC), nitrate (NO<sub>3</sub>), phosphate (PO<sub>4</sub>), oxygen (O<sub>2</sub>), total alkalinity (TALK), and dissolved organic phosphorus (DOP) in addition to temperature (T) and salinity (S). In this study the model uses a stationary flow field, for all experiments, and also for future simulations. This flow field was obtained by a previous optimization run, which determined water mass transports representing all major ocean currents and tracer distributions close to hydrographic data of T, S, DIC, NO<sub>3</sub>, PO<sub>4</sub>, O<sub>2</sub>, and TALK. Production and remineralization of organic matter are not simulated explicitly, but are

treated as sinks and sources of DIC and nutrients using Suess/Martin-type equations [Suess, 1980; Martin *et al.*, 1987],

$$J(x, y, z) = \alpha(x, y) \cdot z^{-\beta(x, y)} \quad z \geq z_{EZ}. \quad (1)$$

[6]  $J(x, y, z)$  is the particle flux at a given location ( $x, y, z$ ), while the functions  $\alpha$  and  $\beta$  describe the export production and the shape of the remineralization curve for each model column. The two parameters,  $\alpha$  and  $\beta$ , have also been optimized by the Adjoint Method for each model column to achieve particle fluxes resulting in property distributions close to the data. At the base of the euphotic zone ( $z_{EZ} = 133$  m) the particle flux  $J$  is equivalent to the export production (EP), which amounts to 10 Gt C per year, globally. There is gas exchange at the sea surface for CO<sub>2</sub> and O<sub>2</sub>. Formation and dissolution of dissolved organic matter (DOM) and calcium carbonate (CaCO<sub>3</sub>) are also included, affecting the concentrations of DIC and, especially the latter, alkalinity.

[7] There are no ocean-atmosphere feedback mechanisms implemented in the model used in this study; that is, the atmosphere strictly follows the prescribed scenario. In fact, large-scale carbon uptake rates as they occur especially in the time-dependent experiments should result in a significant lowering of atmospheric pCO<sub>2</sub>, which in turn (as a negative feedback) would lower the CO<sub>2</sub> gas exchange rates. Therefore the CO<sub>2</sub> uptake rates simulated in our study may be slightly overestimated. The approximation of the potential effect of carbon uptake in the ocean on the atmospheric pCO<sub>2</sub> is calculated separately, whereby sequestration of about 2 Gt C leads to a reduction of atmospheric pCO<sub>2</sub> by about 1 ppm. The calculation is a careful estimate derived from the approximate preindustrial atmospheric carbon content of 600 Gt C [Siegenthaler and Sarmiento, 1993], corresponding to a pCO<sub>2</sub> of about 280 ppm [Nefel *et al.*, 1994]. Using the stationary model flow field also for the future scenarios is somewhat oversimplifying, but it permits the calculation of net effects of changes within the biological cycling of carbon and nutritional elements on the marine carbon budget.

### 2.2. Experiments

[8] Four experiments (I–IV) are carried out to determine the effects of spatial and temporal variations in the C:N composition of sinking POM on the inventory and distribution of DIC in the global ocean. Table 1 gives an overview of the experiments and their key parameters, as,

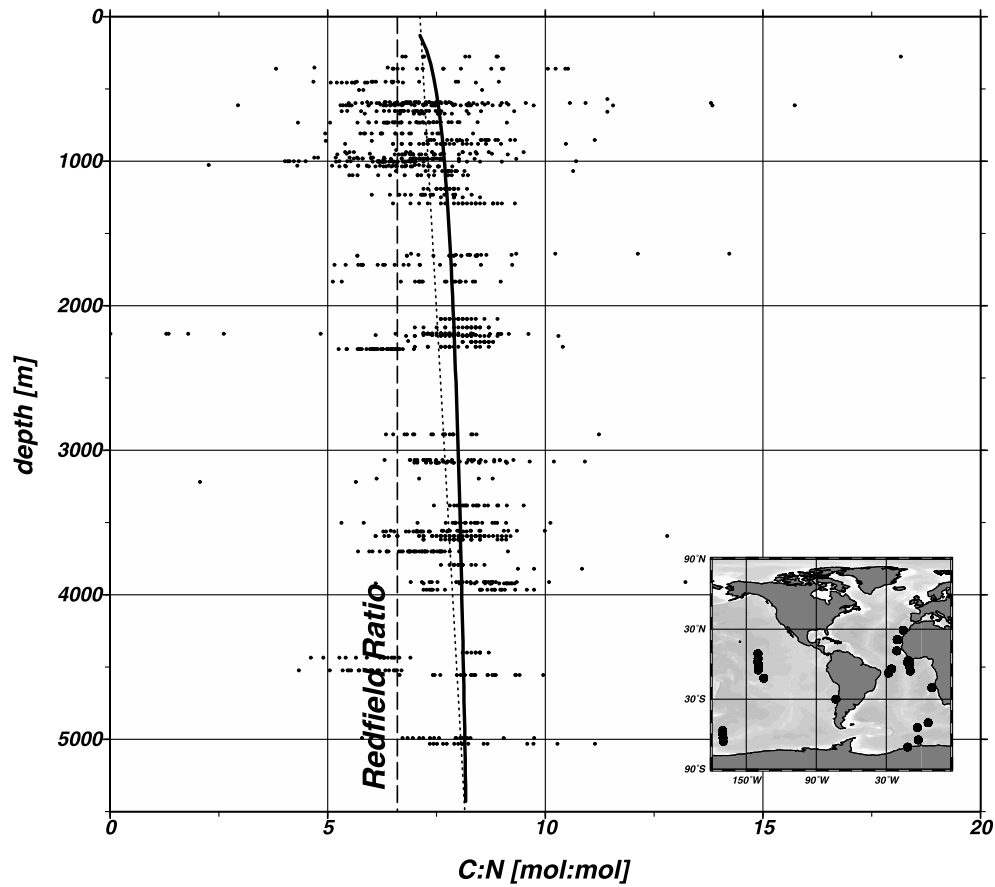


**Figure 1.** C:N ratios of sediment trap samples versus depth. The dashed line indicates the classical RR of C:N (6.6), the dotted line is the linear regression line for the increase of C:N ratios with depth, and the solid line is the C:N ratio of sinking particles as realized in the model (modified from *Schneider et al.* [2003]).

for example, atmospheric pCO<sub>2</sub>, C:N ratio of sinking POM at the base of the euphotic zone ( $z_{EZ}$ ), C:N depth dependence, and the initial fields used for the tracers DIC, NO<sub>3</sub>, PO<sub>4</sub>, O<sub>2</sub>, and TALK.

### 2.2.1. Experiment I

[9] In the first experiment (I) the constant classical RR of 6.6 is applied for the C:N composition of sinking particles. After integration over 5000 years the ocean is in equilibrium with a preindustrial atmosphere of 278 ppm and there is no net CO<sub>2</sub> gas exchange, when integrated over the global ocean. Thus experiment I serves as a reference for a steady-state ocean with particle fluxes corresponding to the constant classical RR.

### 2.2.2. Experiment II

[10] In experiment II the composition of sinking particles is implemented according to the results of *Schneider et al.* [2003]; that is, the C:N ratio of sinking particles at  $z_{EZ}$  is set to 7.1. The C:N depth dependence is realized by adjusting the parameter  $\beta$  (equation (1)), which determines the shape of the particle flux curve for a given element. In contrast to experiment I, where values for  $\beta$  were identical for all elements C, N, and P, the parameter  $\beta$  for carbon ( $\beta_C$ ) is now modified. Hence a factor of 0.963 was empirically determined for modification of  $\beta_C$ , resulting in a depth-dependent curve for the C:N ratios of sinking POM, fitting both the C:N ratios of particles at the base of the euphotic

zone (7.1) and in 5000 m water depth (8.1) as determined by *Schneider et al.* [2003] (Figure 1). After integrating over 8000 years, experiment II is also run into steady state with a preindustrial atmosphere of 278 ppm CO<sub>2</sub>, providing a steady-state solution for an ocean with higher-than-Redfield and depth-dependent C:N composition of sinking particles.

### 2.2.3. Experiment III

[11] Experiment III is a time-dependent simulation calculating the effect of anthropogenic CO<sub>2</sub> emissions on the marine DIC inventory and distribution, which is due to the physical (solubility) carbon uptake, while particle fluxes are implemented temporally constant, as in experiment II (Table 1). The simulation runs from the year 1770 until 2200, starting with the equilibrium tracer field obtained from experiment II. The atmosphere follows the S650 scenario [*Houghton et al.*, 1997], which consists of data taken from ice core records (1770–1950) [*Neftel et al.*, 1994] and the Mauna Loa CO<sub>2</sub> record (1950–1990) [*Keeling and Whorf*, 2002], starting with a preindustrial value of 278 ppm and leading to a maximum of 650 ppm in the year 2200. The time-dependent course of atmospheric pCO<sub>2</sub> is shown in Figure 2.

### 2.2.4. Experiment IV

[12] Experiment IV is the second time-dependent simulation, carried out to determine the impact of CO<sub>2</sub>-dependent element ratios of sinking POM on the marine carbon cycle.

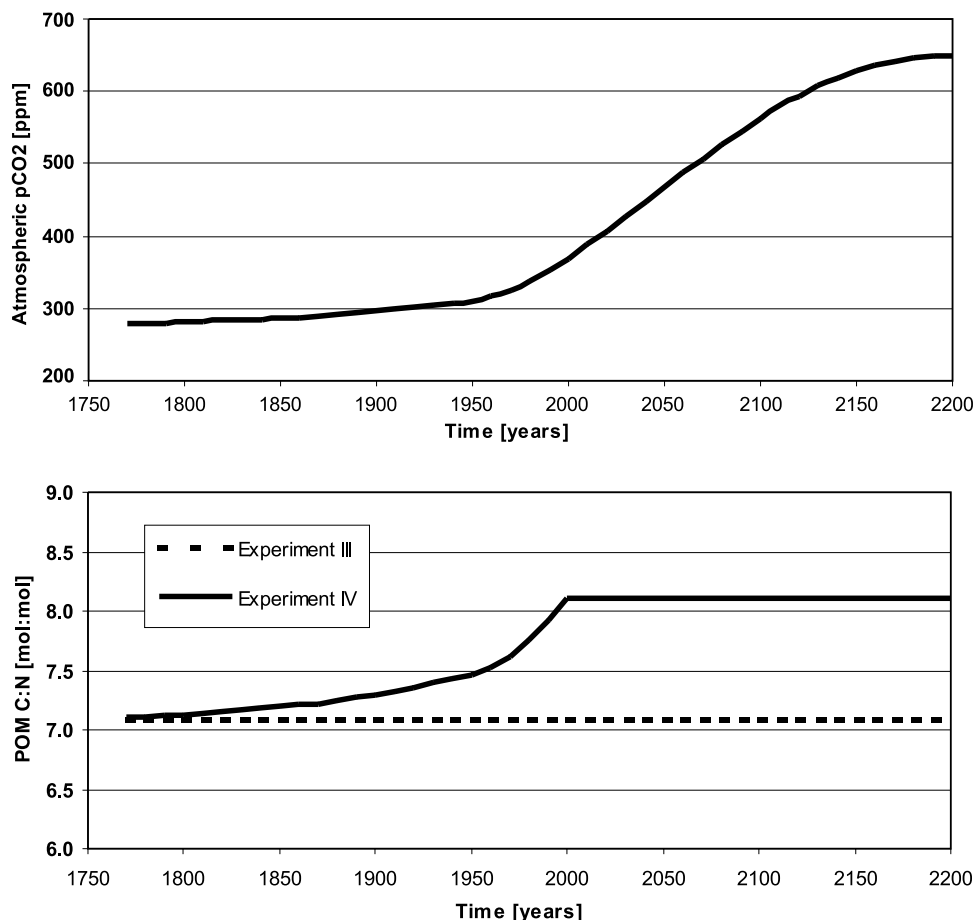


**Figure 2.** Scenario for the (top) atmospheric CO<sub>2</sub> concentration and (bottom) C:N ratios of sinking particles at  $z_{EZ}$  over the simulation interval from 1770–2200.

The assumptions are hypothetical, based on a probable response in the production of transparent exopolymer particles (TEP), which are extracellular particulate carbohydrates, a derived product of primary production of phytoplankton cells [Aldredge *et al.*, 1993; Logan *et al.*, 1995; Passow, 2002]. TEP may play a vital role in future biogeochemical cycles, as the rate of photosynthesis is dependent on the abundance of CO<sub>2</sub> or DIC; this is valid for the TEP production as well [Engel, 2002; Engel *et al.*, 2004]. In contrast to cell growth, TEP production is not primarily nutrient limited, and therefore a general CO<sub>2</sub> dependence can emerge. With a C:N ratio of 20–26 [Engel and Passow, 2001; Mari *et al.*, 2001] this material may cause an enhanced uptake of carbon relative to nutrients [Engel *et al.*, 2002], a fact which is generally referred to as carbon overconsumption in the recent literature [Toggweiler, 1993; Michaels *et al.*, 1994; Marchal *et al.*, 1996].

[13] While in other future simulations of ocean carbon cycle models marine biological production is merely reduced and/or turned off, the current scenario provides a simulation of plausible changes within the biological cycling of elements as a consequence of global change. For this purpose, the C:N ratios of sinking POM at the base of the euphotic zone ( $z_{EZ}$ ) in the model are varied in concert with the atmospheric pCO<sub>2</sub> in a way that beginning with a

preindustrial value of 7.1 they are increasing in a linear relation to the atmospheric pCO<sub>2</sub>, to reach a value of 8.1 in the year 2000. From then on they remain temporally constant. During the entire simulation the C:N depth dependence is kept as in the preceding experiments. The time-dependent course of atmospheric pCO<sub>2</sub> and the corresponding C:N composition of sinking particles at the base of the euphotic zone ( $z_{EZ}$ ) are shown in Figure 2.

[14] By this means, the current model scenario (IV) represents a relative increase in the contribution of TEP to global particle export fluxes by 5% from preindustrial to present times. This is a rather conservative estimate, as, for example, experiments in the Baltic Sea revealed a 25% increase in TEP-production between preindustrial and present CO<sub>2</sub> levels [Engel, 2002]. The experiments also showed more or less constant TEP production beyond the current CO<sub>2</sub> concentration [Engel, 2002], for this reason the temporal evolution of C:N ratios levels off in the year 2000 at a value of 8.1. However, the assumption is still hypothetical, since nutrient limitation appears neither globally nor in every phytoplankton bloom, TEP production varies temporally and spatially in the ocean, but the particular increase lies safely within the range of natural variability, as, for example, the mean C:N ratio of sinking POM in the upper 1000 m of the water column is 7.25 ( $s = 1.46$ ;  $n = 389$ )

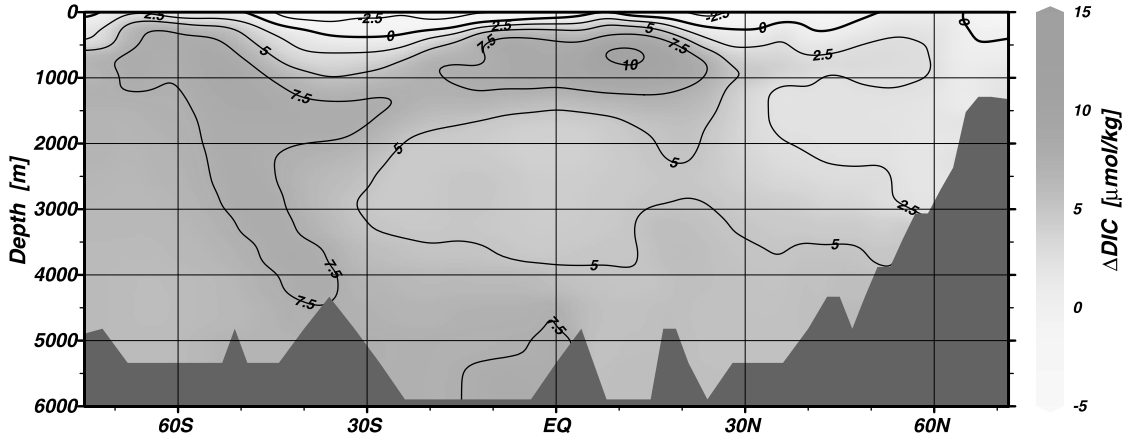


**Figure 3.** Differences in the DIC concentrations ( $\Delta\text{DIC}$ ) between the non-Redfield equilibrium experiment (II) and the RR equilibrium ocean (I) on a north to south transect in the Atlantic Ocean along  $25^\circ\text{W}$ .

Schneider [2003]. Furthermore, from 1770 until 2000 the modeled increase of POM C:N ratios is 0.004 units per year, and during the decades from 1980 until 2000 it amounts to 0.02 units per year, which is still a factor of 10 lower than increases found for sediment trap material from the HOT site (+0.23 units per year) during the years 1989–1995 [Schneider, 2003]. Anyhow, the increasing C:N ratio of particles at  $z_{EZ}$ , as simulated in experiment IV, can be seen as representative for any mechanism leading to changes in CO<sub>2</sub> uptake by the ocean due to variable C:N ratios.

[15] Theoretically, it is also possible to yield a lowering of C:N ratios as a result of global change, for example, by changes in dominating phytoplankton species. Finally, the net effect of global change on the marine carbon cycle will be the sum of several single mechanisms, and the quantification of the net result is beyond the scope of this study.

## 2.3. Results

### 2.3.1. Steady-State Experiments

[16] It has to be mentioned that all results of the current study are model results; that is, all apparent changes in marine carbon and nutrient distributions do not refer to the real ocean, but to our understanding of underlying processes. As the starting field for all tracers in experiment I is obtained by the Adjoint Method and only relatively small deviations from these starting fields occur, the results of the current study represent hydrographic measurements very well, yielding reliable values of carbon and nutrient distributions.

[17] Experiment I provides mean concentrations for the whole model domain of the following tracers:

$$\text{DIC} = 2227 \mu\text{mol kg}^{-1},$$

$$\text{NO}_3 = 31.2 \mu\text{mol kg}^{-1},$$

$$\text{PO}_4 = 2.16 \mu\text{mol kg}^{-1},$$

$$\text{O}_2 = 164 \mu\text{mol kg}^{-1},$$

$$\text{TALK} = 2366 \mu\text{mol kg}^{-1}.$$

[18] In experiment II, the modeled mean DIC concentration over the entire model domain is  $2236 \mu\text{mol kg}^{-1}$ , which is about  $9 \mu\text{mol kg}^{-1}$  higher than results from experiment I. While mean concentrations and spatial distributions of the other tracers remain unchanged, the higher mean DIC value in II corresponds to a higher total ocean DIC inventory of about 150 Gt C, compared to the classical RR steady-state scenario, accompanied by enhanced vertical DIC gradients. There are considerable differences in the DIC concentrations ( $\Delta\text{DIC}$ ) between the two equilibrium experiments (I, II). On a meridional section in the Atlantic Ocean along  $25^\circ\text{W}$  (Figure 3) the deep ocean exhibits elevated DIC concentrations everywhere on the transect, whereas large areas of the sea surface show lower DIC concentrations in experiment II compared to experiment I. These changes are caused by an increased strength of the biological carbon pump, forced by the lower  $\beta_C$ , which leads to a more effective downward carbon transport.

[19] The distribution of apparently higher DIC concentrations in experiment II compared to experiment I (Figure 3) reflects the general pattern of water mass circulation in the Atlantic Ocean, where gradually increasing DIC concentrations highlight the spreading of North Atlantic Deep Water (NADW) down and southward, and also the Antarctic Intermediate Water (AAIW) in its northward direction. In the South Atlantic, there is upwelling of DIC enriched deep water leading to significantly higher surface water DIC concentrations between  $50^\circ\text{S}$  and  $65^\circ\text{S}$ . Even though there is no net flux of CO<sub>2</sub> between ocean and atmosphere in experiment II, lower surface water DIC concentrations in areas of deep water formation and higher concentrations at the sea surface in upwelling regions will lead to a higher total CO<sub>2</sub> gas exchange; that is, the cycling of CO<sub>2</sub> between

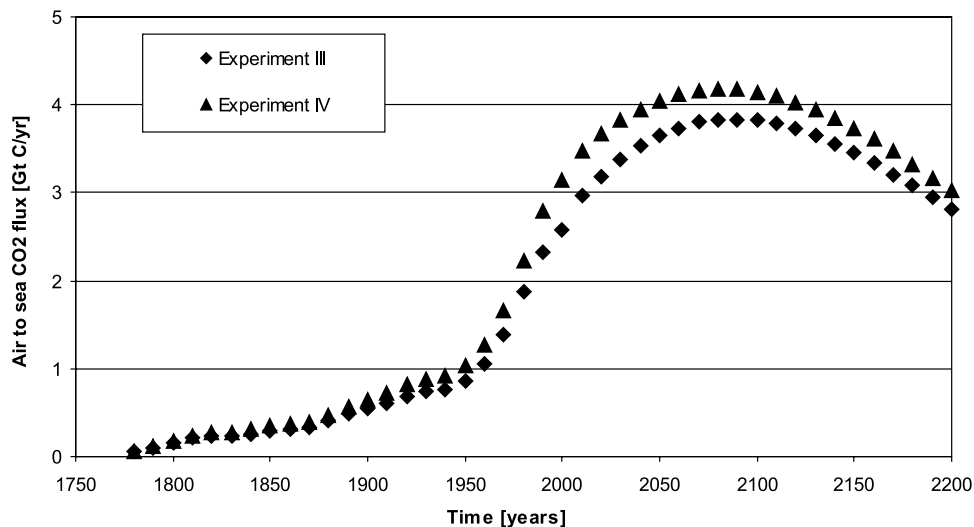


**Figure 4.** Annual net air-sea fluxes of CO<sub>2</sub> in the experiments III (diamonds) and IV (triangles).

atmosphere and ocean is accelerated in experiment II, if compared to experiment I.

[20] The differences in the concentrations and vertical gradients of DIC between the two steady-state experiments are low compared to the high background concentration of DIC in the ocean (+0.5%). Most probably, differences between the two scenarios (I, II) cannot be detected by measurements because of relatively large natural variability and analytical inaccuracies. By representing the elemental composition of marine particle fluxes as determined by recent data analyses from sediment trap material, experiment II has shown that compared to particulate nitrogen flux, there is a more effective downward transport of carbon by sinking POM. Consequently, models using the classical RR and depth-independent particle compositions will underestimate the strength of the biological carbon pump, and

accordingly the marine carbon inventory and vertical DIC gradients as well.

### 2.3.2. Time-Dependent Simulations

[21] In the time-dependent simulations (III, IV) the atmospheric pCO<sub>2</sub> is prescribed to increase from the preindustrial (1770) value of 278 ppm to a maximum of 650 ppm in the year 2200 [Houghton *et al.*, 1997]. While during the first 200 years of the simulation the increase of atmospheric pCO<sub>2</sub> from 278 to 310 ppm is moderate, it is growing more rapidly after 1950 (Figure 2). The corresponding anthropogenic CO<sub>2</sub> (aCO<sub>2</sub>) uptake by the ocean due to solubility and deep water formation only (III) is low and increasing slightly from 1770 to 1950, reaching a flux of about 1 Gt C/yr in 1950 (Figure 4). From then on, the air-sea aCO<sub>2</sub> fluxes increase faster to about 2.6 Gt C in the year 2000, forced by rapidly rising atmospheric pCO<sub>2</sub> after 1950.

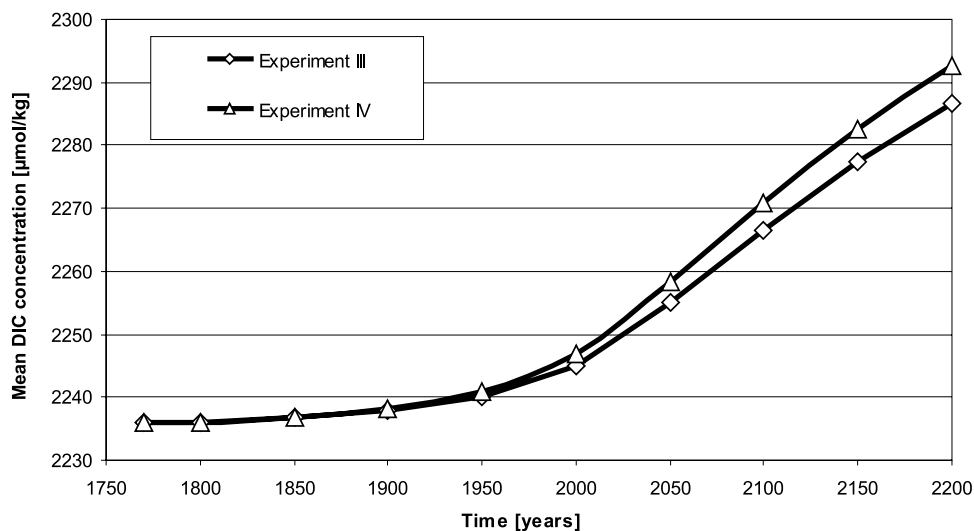


**Figure 5.** Increase of the global mean DIC concentrations in  $\mu\text{mol kg}^{-1}$  for the experiments III (diamonds) and IV (triangles).

In the year 2080, maximum fluxes of about 3.8 Gt C per year are reached. Farther on, air-sea aCO<sub>2</sub> fluxes are still positive, but decreasing evoked by a less steep increase of the atmospheric pCO<sub>2</sub> after 2080.

[22] The net uptake of aCO<sub>2</sub> by the ocean is followed by continuously rising mean DIC concentrations, shown in Figure 5. From preindustrial to the year 2000 the mean oceanic DIC concentration is simulated to increase from about 2236 μmol kg<sup>-1</sup> DIC to 2245 μmol kg<sup>-1</sup>, and farther on to 2287 μmol kg<sup>-1</sup> in the year 2200. This increase is not evenly distributed over the global ocean, but is related to the general oceanic circulation pattern. Figure 6 shows, on a north to south section along 25°W in the Atlantic Ocean, the changes of DIC concentrations between given times of the simulation (1800, 1900, 2000, and 2100) and preindustrial values (experiment II), which represent the respective aCO<sub>2</sub> concentrations as simulated by experiment III. As expected, at all times the strongest aCO<sub>2</sub> uptake occurs at the sea surface, where gas exchange takes place. In the year 1800, surface water aCO<sub>2</sub> concentrations are low (~1 μmol kg<sup>-1</sup>), and the water masses below 1000 m depth are virtually unaffected. In the year 1900, there are already 10–12 μmol kg<sup>-1</sup> aCO<sub>2</sub> simulated for the Atlantic surface waters. The aCO<sub>2</sub> concentrations decrease gradually along the pathway of the North Atlantic Deep Water (NADW), which forms in the Nordic and Labrador Seas and flows southward at a depth of 1000–3000 m, transporting the aCO<sub>2</sub> signal into the ocean's interior. Equatorial upwelling and upwelling in the Southern Ocean cause a shallowing of the aCO<sub>2</sub> isolines close to the surface. In the year 2000 the surface water aCO<sub>2</sub> concentrations in the North Atlantic amount to 40–50 μmol kg<sup>-1</sup>, and there are about 10 μmol kg<sup>-1</sup> in the North Atlantic Deep Water on 30°N in 2000 m water depth. Until the year 2100 the basic pattern of aCO<sub>2</sub> uptake remains the same, but the model predicts surface water values of about 140 μmol kg<sup>-1</sup>, which corresponds to an increase in the surface ocean DIC concentration of about 7% compared to preindustrial values.

[23] In experiment IV the net annual air-sea flux of CO<sub>2</sub> follows basically the same pattern as in experiment III (Figure 4). However, the temporally increasing C:N ratios of sinking POM from 1770 to 2000 lead to elevated aCO<sub>2</sub> fluxes across the air-sea interface, especially after 1950. In the year 2000 the aCO<sub>2</sub> flux amounts to 3.1 Gt C/yr, which is about 0.5 Gt C higher than compared to experiment III, reaching its maximum also in the year 2080 with 4.2 Gt C/yr (+0.3 Gt C). The higher air-sea aCO<sub>2</sub> flux in experiment IV is followed by a stronger increase in the mean DIC inventory, which in the year 2000 (2200) is simulated to be 2 μmol kg<sup>-1</sup> (6 μmol kg<sup>-1</sup>) higher than in experiment III, equivalent to a higher carbon accumulation of about 30 Gt (100 Gt).

[24] The net effect of CO<sub>2</sub>-dependent POM compositions on the marine carbon budget, ΔaCO<sub>2</sub>, is the difference in the DIC concentration between the experiments III and IV (IV – III), which is calculated for the years 1800, 1900, 2000, and 2100 on a meridional section along 25°W in the Atlantic Ocean (Figure 7). There are large ocean areas of significant impact: While at the sea surface DIC concentrations are lower in experiment IV, especially in the subtropics, there

are generally higher DIC concentrations in the ocean's interior at all times. Particularly in the lower latitudes of the Atlantic Ocean, there is a strong increase of DIC located in the subsurface waters from closely beneath the surface until 1000 m depth. Compared to the amount of aCO<sub>2</sub> uptake by solubility only (III, Figure 6), the additional effects of CO<sub>2</sub>-dependent element ratios are smaller by a factor of 10, and compared to the high background concentration of DIC in the ocean, these effects are negligible for the oceanic carbon budget. If present already, such effects will most probably not be detectable by measurements. However, on timescales of decades to centuries the cumulative effect and its potential feedback on atmospheric pCO<sub>2</sub> is substantial, as, for example, the CO<sub>2</sub>-dependent POM composition accounts on global average for another 30 and 100 Gt C, accumulated in the ocean until the years 2000 and 2200, respectively.

### 3. Discussion

#### 3.1. Ocean Carbon Inventory and Uptake of Anthropogenic CO<sub>2</sub>

[25] Our model experiments showed that the implementation of a moderate shift of C:N ratios of POM above the classical RR clearly influences the model based estimation of the oceanic DIC inventory and its distribution. Specifically, if the C:N of POM are allowed to adopt values, such as determined by *Schneider et al.* [2003], changes in the total oceanic DIC of about 150 Gt C and stronger vertical gradients occur (Figure 3), if compared to a classical RR steady-state scenario. Hence there is a higher efficiency of carbon transport from the surface into the deep ocean, as determined by models with depth-independent particle elemental compositions.

[26] Assuming that these particle compositions exist in a steady-state ocean, especially at preindustrial times, means that there is currently no impact on the oceanic sequestration of anthropogenic CO<sub>2</sub> due to deviations from the classical RR. Considerable effects are merely expected to occur by temporal (CO<sub>2</sub>-dependent) variations in the elemental composition of sinking POM. However, there is a persistent effect of the C:N depth dependence on the total atmospheric CO<sub>2</sub> concentration. The distinction between the two effects, higher-than-Redfield (7.1) and depth-dependent C:N ratios of sinking POM (+0.2 ± 0.1 per km), has revealed that approximately 45 Gt C (30%) of the increased carbon inventory in experiment II are due to the deeper carbon remineralization. For details about the differentiation of both effects, see *Schneider* [2003]. While the amount of DIC increase due to the higher-than-Redfield C:N ratio is strongly dependent on the particular deviation from the RR, the effect of the C:N depth dependence appears, irrespective of the actual value of C:N ratios of sinking POM at z<sub>EZ</sub>. Hence the C:N depth dependence has the potential to reduce the ambient atmospheric pCO<sub>2</sub> by about 20 ppm, a reduction which is effective even in steady state. The amount of 20 ppm reduction agrees very well with results from *Shaffer et al.* [1999], although in their study, different depth-dependent carbon-to-nitrogen remineralization rates in a simple box-model are used. However, in our study the

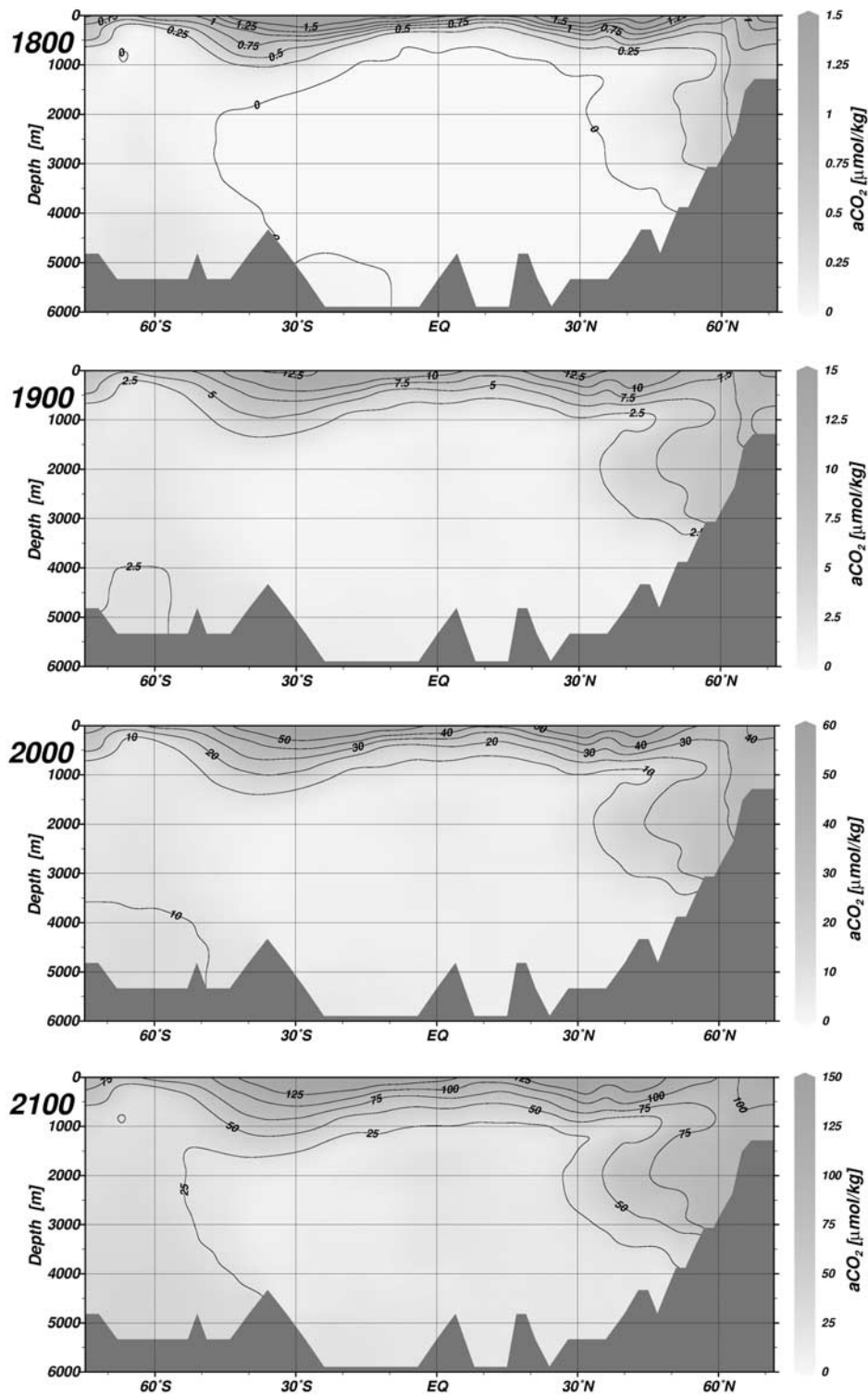


**Figure 6.** Total anthropogenic CO<sub>2</sub> (aCO<sub>2</sub>) concentrations as simulated in experiment III for different times (1800, 1900, 2000, and 2100), displayed on a meridional section along 25°W in the Atlantic Ocean, showing the general pattern of carbon sequestration. Note that the scales for the different panels are different by factors of 10 to 100.

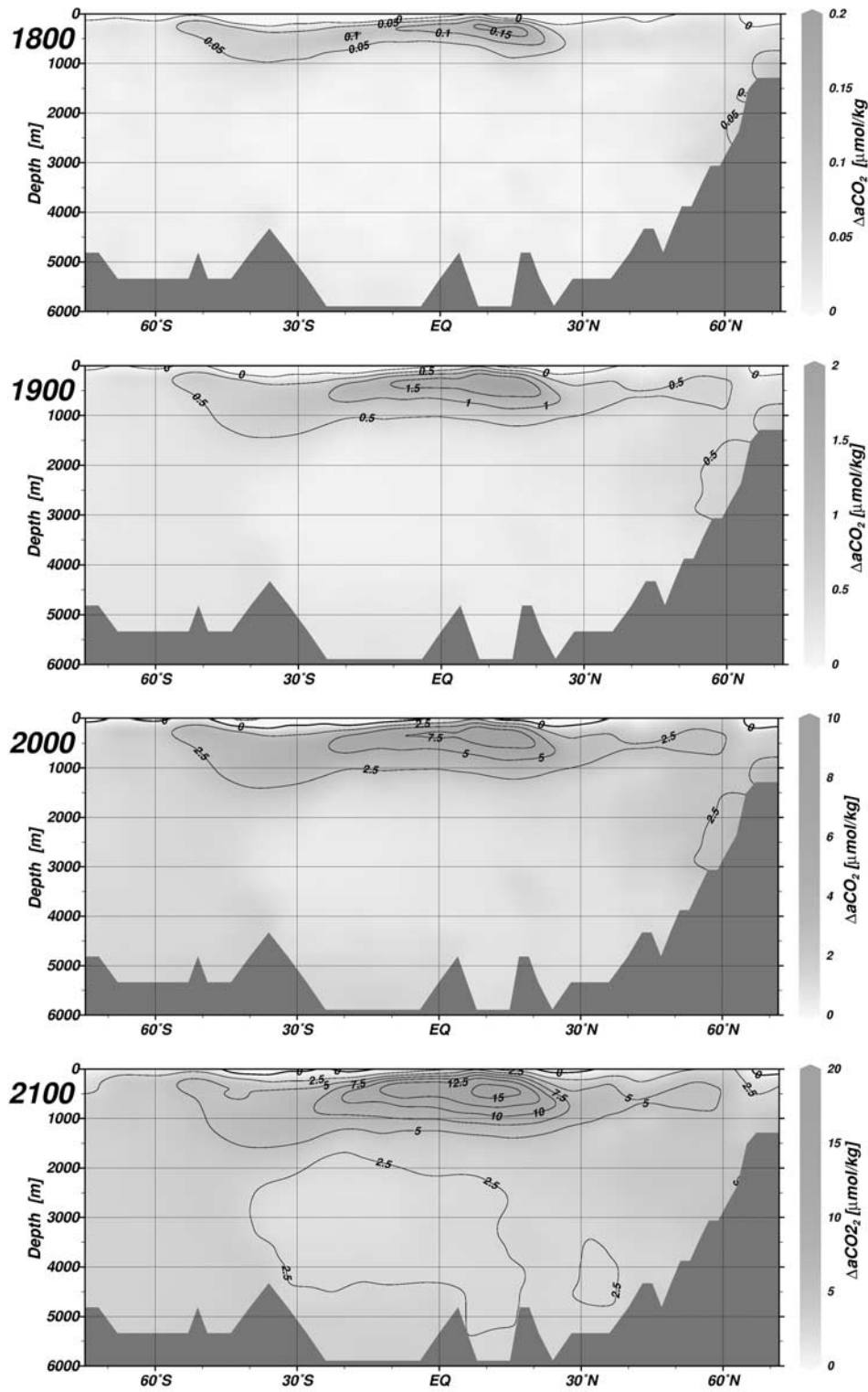


**Figure 7.** Net anthropogenic CO<sub>2</sub> ( $\Delta a\text{CO}_2$ ) concentrations induced by CO<sub>2</sub>-dependent particle compositions as simulated in experiment IV (difference between results from experiments III and IV) on a meridional section along 25°W in the Atlantic Ocean. Note that there is no uniform scaling for the different plots.

**Table 2.** Cumulated CO<sub>2</sub> Uptake of the Ocean in Gt C for Experiments III and IV From Preindustrial to Present Times (2000) and for Each of the Two Future Centuries Beginning in the Years 2000 and 2100<sup>a</sup>

Experiment	1770–2000	2000–2100	2100–2200
III	152	352	341
IV	182 (+30)	392 (+40)	368 (+27)

<sup>a</sup>The numbers in parentheses denote the additional uptake in experiment IV, compared to experiment III, for each of the given time intervals.

spatial distribution of simulated aCO<sub>2</sub> in the ocean can also be evaluated.

[27] The rates of anthropogenic CO<sub>2</sub> (aCO<sub>2</sub>) uptake and its distribution in the ocean as obtained by both experiments III and IV in the current study also agree well with results from other studies, model experiments [Orr *et al.*, 2001], and measurement-based estimates [Gruber, 1998; Körtzinger *et al.*, 1999]. However, the net effect of additional carbon sequestration due to CO<sub>2</sub>-dependent particle compositions ( $\Delta$ aCO<sub>2</sub>) on marine DIC concentrations (Figure 7) is a factor of 10 lower than the amount of total aCO<sub>2</sub> uptake obtained by solubility only (Figure 6) and lies within the range of errors of measurement-based estimates, which are about  $\pm 10 \mu\text{mol kg}^{-1}$  [Körtzinger *et al.*, 1999]. Moreover, seasonal and interannual variations in marine DIC concentrations are on the order of magnitude of 20–100  $\mu\text{mol kg}^{-1}$  [Gruber *et al.*, 2002; Wong *et al.*, 2002]; that is, the additional effect on the marine carbon reservoir as computed in experiment IV is (1) very low compared to the high background DIC concentration in the ocean and (2) likely to be hidden by analytical inaccuracies and natural variability. Nevertheless, the simulated additional annual air-sea flux of aCO<sub>2</sub> in experiment IV, especially after the year 1950, and the resulting cumulative aCO<sub>2</sub> uptake on timescales of decades to a few hundred years is substantial. For example, the simulated air-sea aCO<sub>2</sub> flux for the year 2000 is 0.5 Gt C/yr higher in IV than in III, complying with the error for estimates of the actual uptake of anthropogenic CO<sub>2</sub> by the ocean [Houghton *et al.*, 2001]. Most importantly, with a surplus of 100 Gt C accumulated in experiment IV over the entire simulation period (1770–2200), the aCO<sub>2</sub> uptake is considerably higher than in experiment III. This could lead to a reduced increase in the atmospheric pCO<sub>2</sub> by about 50 ppm, which is a tremendous effect, for example, compared to the glacial-interglacial atmospheric pCO<sub>2</sub> variation of 100 ppm [Barnola *et al.*, 1999].

[28] Table 2 shows the accumulated aCO<sub>2</sub> uptake in Gt C for the experiments III and IV, divided into the time intervals from preindustrial to present (2000), where C:N ratios are increasing in experiment IV, and for the future two centuries (2000–2100 and 2100–2200), where in both experiments the C:N ratios of sinking POM are temporally constant. In the first interval, there is a 30 Gt C higher net uptake in experiment IV, which corresponds to an increase of about 20% of the amount obtained by experiment III and which may reduce the atmospheric pCO<sub>2</sub> by approximately 15 ppm. For the future 100 years (2000–2100), the simulation yields a relative decrease in the additional uptake by

experiment IV. However, there is still a 40 Gt C higher uptake in IV from 2000 until 2100; that is, this process is still able to sustain a 10% higher aCO<sub>2</sub> uptake as obtained by temporally constant C:N ratios of POM (III). In the last simulated centennial (2100–2200), there is also a higher uptake of aCO<sub>2</sub> in IV, accumulating about 27 Gt C more than during the same interval in experiment III. The reason for the later decreasing contribution of the C:N variability is the temporal constancy of C:N ratios of POM after the year 2000, while at the same time there is a higher contribution of CO<sub>2</sub> solubility to the total carbon uptake as response to further increasing atmospheric pCO<sub>2</sub>.

[29] In summary, higher-than-Redfield and depth-dependent C:N ratios of sinking POM as determined by Schneider *et al.* [2003] lead in a steady-state ocean to a slight increase (0.5%) of the total DIC inventory, compared to a steady-state ocean assuming particle compositions following the constant classical RR. The important aspect of this result is the occurrence of stronger vertical DIC gradients, which may be undetectable at present by DIC measurements, but which have the potential to lower the prevalent atmospheric pCO<sub>2</sub> by about 20 ppm, permanently. The additional effect of CO<sub>2</sub>-dependent C:N ratios of sinking POM on the sequestration of anthropogenic CO<sub>2</sub> in the ocean is even smaller compared to the oceanic carbon reservoir. The hypothesized C:N variation lies within the range of natural variability, but its cumulative contribution on oceanic aCO<sub>2</sub> sequestration is substantial on decadal to centennial timescales. Thus any mechanism providing a systematic increase of C:N ratios of sinking POM as in experiment IV is able to increase air-sea aCO<sub>2</sub> fluxes permanently by 10–20% and thereby has the potential for a considerable reduction of the atmospheric pCO<sub>2</sub>.

### 3.2. Variable Element Ratios of POM and Global Change

[30] As explained above, our model experiments have shown that currently no effects on the oceanic sequestration of anthropogenic CO<sub>2</sub> (aCO<sub>2</sub>) can be expected due to non-Redfield element ratios of sinking particles, unless temporal (CO<sub>2</sub>-dependent) variations occur. There are, however, a number of reasons why CO<sub>2</sub>-dependent variations in marine biological production are very likely to emerge and can even be present already (Figure 8). A rise in the global mean air temperature during the last century has already been detected and is partly attributed to human influence [Houghton *et al.*, 2001], and there is general agreement about expected impacts on large-scale ocean circulation. However, assumptions about changes in marine biological productivity on global scale are highly speculative, and it is likely that feasible changes at present are hidden by natural variability.

[31] Probable impacts of global change on marine carbon sequestration, mainly due to changes in ocean circulation, have been estimated by a number of model studies [Maier-Reimer *et al.*, 1996; Sarmiento and Le Quéré, 1996; Sarmiento *et al.*, 1998; Sarmiento and Hughes, 1999; Matear and Hirst, 1999; Friedlingstein *et al.*, 2001; Bopp *et al.*, 2001]. These studies agree that global warming heats the surface ocean and thus intensifies stratification. Both

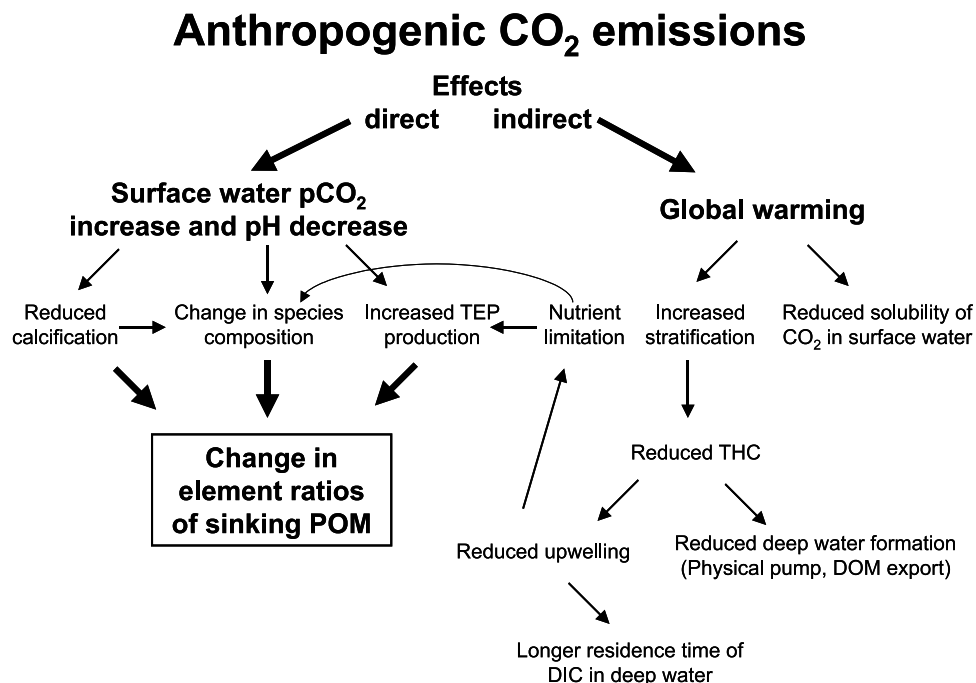


**Figure 8.** Global change: direct and indirect effects of anthropogenic CO<sub>2</sub> emissions on marine physical and biogeochemical properties. POM, particulate organic matter; DOM, dissolved organic matter; TEP, transparent exopolymer particles; THC, thermohaline circulation; DIC, dissolved inorganic carbon.

effects, independently, lead to a decrease in oceanic carbon uptake, as surface heating reduces the CO<sub>2</sub> solubility and a stronger stratification reduces deep water formation and thereby export of dissolved organic and inorganic carbon. Next to the occurrence of physical changes, effects on the ocean's biology are assumed in some of the models by means of decreased biological production, as reduced overturning leads to less upwelling of nutrients, reducing new production and presumably export fluxes. The amount of reduced carbon uptake differs between the different studies depending on the type of model and atmospheric pCO<sub>2</sub> scenario used. The results range from 26 to 200 Gt C, which are predicted to be taken up less compared to the carbon uptake under steady-state circulation until the year 2100.

[32] There are, however, no global estimates of changes in the oceanic carbon uptake due to direct effects on marine biology. However, generally, elevated pCO<sub>2</sub> in the surface water leads to shifts in chemical equilibria and the carbonate system, as, for example, a lowering of surface water pH [Wolf-Gladrow *et al.*, 1999], affecting biological production. Calcification of the dominant planktonic carbonate species is reported to decrease with increasing pCO<sub>2</sub>, a fact which is accompanied by a decreasing PIC:POC ratio [Riebesell *et al.*, 2000; Zondervan *et al.*, 2001]. The lower PIC:POC ratio is not only due to reduced calcification, but also affected by increased POC production of the individual cells [Riebesell *et al.*, 2001; Zondervan *et al.*, 2002]. Theoretically, both effects, reduced calcification and increased POC production can counteract increasing pCO<sub>2</sub> in the surface ocean.

[33] In practice, some field measurements of changing element ratios of POM and DOM can be interpreted as probable future developments due to global change. Arrigo *et al.* [1999] found that the phytoplankton community structure of the Southern Ocean might shift as a consequence of increased stratification resulting from global warming and increased precipitation. From the Ross Sea they reported a dominance of diatoms in more stratified waters over phaeocystis which dominate in more deeply mixed water masses. Even though phaeocystis seem to be able to drawdown CO<sub>2</sub> more efficiently from the atmosphere than diatoms, the latter are supposed to be more important for sedimentation. Anyhow, such local shifts in the community structure of phytoplankton may change the large sink for anthropogenic CO<sub>2</sub> in the Southern Ocean. In the subtropical North Pacific Ocean, changes in the elemental composition of DOM over the last decade have been observed by Church *et al.* [2002]. At the HOT time series station during the last 10 years, there was a significant increase in DOC production, raising the C:P ratios of DOM noticeably. While small and insignificant changes in the DOC:DON and DON:DOP ratios were measured, they found an increase in the DOC:DOP ratio of 17% from 408 to 478 molar units. These findings were explained with a recent reorganization of the plankton community dynamics as a consequence of global change [Church *et al.*, 2002].

[34] Even though the model approach (IV) in the current study does not account for changes in the physical properties of the ocean, in contrast to the models mentioned above, a possible response of marine biological production to global change is examined. In this way it is possible to

isolate a probable net effect of ocean biology, however, showing that this example of enhanced biological carbon drawdown cannot compensate the reduced CO<sub>2</sub> uptake rates as predicted by other models. It rather alleviates decreases of the physical pump, for example, by 75% compared to the results of *Matear and Hirst* [1999].

[35] We summarize, that other model scenarios for the future predict that there are changes in ocean circulation patterns leading to higher stratification and thus nutrient limitation, suggesting reduced oceanic carbon uptake. However, on the other hand, parts of marine biological production may benefit from the changes. For example, the moderate change of C:N element ratios of POM in the current study revealed that biological production has a strong potential for changes in ocean carbon uptake including substantial consequences on the atmospheric pCO<sub>2</sub>. Hence there are a number of indications that the marine carbon cycle is currently not in steady state, and the net effect on global oceanic carbon sequestration is yet highly speculative.

### 3.3. Conclusions

[36] • Higher-than-Redfield and depth-dependent C:N ratios of sinking particles lead to a higher DIC inventory and to stronger vertical DIC gradients in the ocean compared to estimates using depth-independent element ratios.

[37] • The C:N depth dependence of marine sinking particles has the potential to reduce the ambient atmospheric pCO<sub>2</sub> by about 20 ppm, permanently.

[38] • Even moderate temporal (CO<sub>2</sub>-dependent) changes in the C:N elemental composition of marine sinking particles, which are on the order of magnitude of natural variability, have important effects on the marine carbon budget. While the impact on the inventory and distribution of DIC in the ocean is low compared to the high marine background DIC concentration, the cumulative effect on the uptake and storage of anthropogenic CO<sub>2</sub> in the ocean on timescales of decades to centuries is substantial.

[39] • Any mechanism leading to CO<sub>2</sub>-dependent changes in the C:N ratios of sinking particles as simulated in our example study may counteract the predicted decreasing anthropogenic CO<sub>2</sub> sequestration due to a reducing physical pump (solubility, deep water formation). Compensation of anthropogenic CO<sub>2</sub> emissions, however, will not be achieved.

[40] • More information about direct and indirect CO<sub>2</sub> dependencies of marine biological production on a global scale will be needed to allow better future predictions of climate change.

### References

- Allredge, A., U. Passow, and B. Logan (1993), The abundance and significance of a class of large, transparent organic particles in the ocean, *Deep Sea Res.*, *40*, 1131–1140.
- Arrigo, K. R., D. H. Robinson, D. L. Worthen, R. B. Dunbar, G. R. Di Tullio, M. Van Woert, and M. P. Lizotte (1999), Phytoplankton community structure and the drawdown of nutrients and CO<sub>2</sub> in the Southern Ocean, *Science*, *283*, 365–367.
- Banse, K. (1974), The nitrogen-to-phosphorus ratio in the photic zone of the sea and the elemental composition of the plankton, *Deep Sea Res.*, *21*, 767–771.
- Bamola, J., D. Raynaud, C. Lorius, and N. Barkov (1999), Historical CO<sub>2</sub> record from the Vostok ice core, in *Trends: A Compendium of Data on Global Change*, Carbon Dioxide Inf. Anal. Cent., Oak Ridge Natl. Lab., Oak Ridge, Tenn.
- Bopp, L., P. Monfray, O. Aumont, J. L. Dufresne, H. Le Treut, G. Madec, L. Terray, and J. C. Orr (2001), Potential impact of climate change on marine export production, *Global Biogeochem. Cycles*, *15*, 81–99.
- Church, M. J., H. W. Ducklow, and D. M. Karl (2002), Multiyear increase in dissolved organic matter inventories at Station ALOHA in the North Pacific Subtropical Gyre, *Limnol. Oceanogr.*, *47*, 1–10.
- Engel, A. (2002), Direct relationship between CO<sub>2</sub> uptake and transparent exopolymer particles production in natural phytoplankton, *J. Plankton Res.*, *24*(1), 49–53.
- Engel, A., and U. Passow (2001), Carbon and nitrogen content of transparent exopolymer particles (TEP) in relation to their alcin blue adsorption, *Mar. Ecol. Prog. Ser.*, *219*, 1–10.
- Engel, A., S. Goldthwait, U. Passow, and A. Alldredge (2002), Temporal decoupling of carbon and nitrogen dynamics in a mesocosm diatom bloom, *Limnol. Oceanogr.*, *47*, 753–761.
- Engel, A., B. Delille, S. Jacquet, U. Riebesell, E. Rochelle-Newall, A. Terbrüggen, and I. Zondervan (2004), TEP and DOC production by *emiliania huxleyi* exposed to different CO<sub>2</sub> concentrations: A mesocosm experiment, *Aquat. Microb. Ecol.*, *34*, 93–104.
- Friedlingstein, P., L. Bopp, J. L. Dufresne, L. Fairhead, H. Le Treut, P. Monfray, and J. Orr (2001), Positive feedback between future climate change and the carbon cycle, *Geophys. Res. Lett.*, *28*(8), 1543–1546.
- Gruber, N. (1998), Anthropogenic CO<sub>2</sub> in the Atlantic Ocean, *Global Biogeochem. Cycles*, *12*, 165–191.
- Gruber, N., C. D. Keeling, and N. R. Bates (2002), Interannual variability in the North Atlantic Ocean carbon sink, *Science*, *298*, 2374–2378.
- Houghton, J. T., L. G. Meira Filho, D. J. Griggs, and K. Maskell (1997), Stabilization of atmospheric greenhouse gases: Physical, biological and socioeconomic implications, technical report, Intergov. Panel on Clim. Change, World Meteorol. Org., Geneva.
- Houghton, J. T., Y. Ding, D. J. Griggs, M. Noguer, P. J. van der Linden, and D. E. Xiaosu (2001), *Climate Change 2001: The Scientific Basis. Contribution of Working Group I to the Third Assessment Report of the Intergovernmental Panel on Climate Change (IPCC)*, Cambridge Univ. Press, New York.
- Keeling, C., and T. Whorf (2002), Atmospheric CO<sub>2</sub> records from sites in the SIO air sampling network, in *Trends: A Compendium of Data on Global Change*, Carbon Dioxide Inf. Anal. Cent., Oak Ridge Natl. Lab., Oak Ridge, Tenn.
- Körtzinger, A., M. Rhein, and L. Mintrop (1999), Anthropogenic CO<sub>2</sub> and CFCs in the North Atlantic Ocean: A comparison of man-made tracers, *Geophys. Res. Lett.*, *26*(14), 2065–2068.
- Körtzinger, A., W. Koeve, P. Köhler, and L. Mintrop (2001), C:N ratios in the mixed layer during the productive season in the northeast Atlantic Ocean, *Deep Sea Res.*, *48*, 661–688.
- Logan, B., U. Passow, A. Alldredge, H.-P. Grossart, and M. Simon (1995), Rapid formation and sedimentation of large aggregates is predictable from coagulation rates (half-lives) of transparent exopolymer particles (TEP), *Deep Sea Res.*, *42*, 203–214.
- Maier-Reimer, E., U. Mikolajewicz, and A. Winguth (1996), Future ocean uptake of CO<sub>2</sub>: Interaction between ocean circulation and biology, *Clim. Dyn.*, *12*, 63–90.
- Marchal, O., P. Monfray, and N. R. Bates (1996), Spring-summer imbalance of dissolved inorganic carbon in the mixed layer of the northwestern Sargasso Sea, *Tellus, Ser. B*, *48*, 115–134.
- Mari, X., S. Beauvais, R. Lemée, and M. Pedrotti (2001), Non-Redfield C:N ratio of transparent exopolymeric particles in the northwestern Mediterranean Sea, *Limnol. Oceanogr.*, *46*, 1831–1836.
- Martin, J. H., G. A. Knauer, D. M. Karl, and W. W. Broenkow (1987), VERTEX: Carbon cycling in the northeast Pacific, *Deep Sea Res.*, *34*, 267–286.
- Matear, R. J., and A. C. Hirst (1999), Climate change feedback on the future CO<sub>2</sub> uptake, *Tellus, Ser. B*, *51*, 722–733.
- Michaels, A. F., N. R. Bates, K. O. Buesseler, C. A. Carlson, and A. H. Knap (1994), Carbon-cycle imbalances in the Sargasso Sea, *Nature*, *372*, 537–540.
- Neffel, A., H. Friedli, E. Moor, H. Löttscher, H. Oeschger, U. Siegenthaler, and B. Stauffer (1994), Historical CO<sub>2</sub> record from the Siple Station ice core, in *Trends: A Compendium of Data on Global Change*, Carbon Dioxide Inf. Anal. Cent., Oak Ridge Natl. Lab., Oak Ridge, Tenn.
- Orr, J. C., et al. (2001), Estimates of anthropogenic carbon uptake from four three-dimensional global ocean models, *Global Biogeochem. Cycles*, *15*, 43–60.
- Passow, U. (2002), Transparent exopolymer particles (TEP) in aquatic environments, *Prog. Oceanogr.*, *55*, 287–333.

- Redfield, A. C., B. C. Ketchum, and F. A. Richards (1963), The influence of organisms on the composition of sea water, in *The Sea*, vol. 2, edited by N. Hill, pp. 26–77, Wiley Intersci., Hoboken, N. J.
- Riebesell, U., I. Zondervan, B. Rost, P. D. Tortell, R. E. Zeebe, and F. M. M. Morel (2000), Reduced calcification of marine plankton in response to increased atmospheric CO<sub>2</sub>, *Nature*, 407, 364–367.
- Riebesell, U., I. Zondervan, B. Rost, and R. E. Zeebe (2001), Effects of increasing atmospheric CO<sub>2</sub> on phytoplankton communities and the biological carbon pump, *Global Change Newsl.*, 47, 12–15.
- Sarmiento, J. L., and T. M. C. Hughes (1999), Anthropogenic CO<sub>2</sub> uptake in a warming ocean, *Tellus, Ser. B*, 51, 560–561.
- Sarmiento, J. L., and C. Le Quéré (1996), Oceanic carbon dioxide uptake in a model of century-scale global warming, *Science*, 274, 1346–1350.
- Sarmiento, J. L., T. M. C. Hughes, R. J. Stouffer, and S. Manabe (1998), Simulated response of the ocean carbon cycle to anthropogenic climate warming, *Nature*, 393, 245–249.
- Schlitzer, R. (2000), Applying the adjoint method for global biogeochemical modeling, in *Inverse Methods in Biogeochemical Cycles*, *Geophys. Monogr. Ser.*, vol. 114, edited by P. Kasibhatla et al., pp. 107–124, AGU, Washington, D. C.
- Schlitzer, R. (2002), Carbon export fluxes in the Southern Ocean: Results from inverse modeling and comparison with satellite based estimates, *Deep Sea Res.*, 49, 1623–1644.
- Schlitzer, R. (2004), Export production in the equatorial and North Pacific derived from dissolved oxygen, nutrient and carbon data, *J. Oceanogr.*, 60(1), 53–62.
- Schneider, B. (2003), Variable C:N ratios of particulate organic matter and their influence on the marine carbon cycle, in *Reports on Polar and Marine Research*, vol. 437, Alfred Wegener Inst., Bremerhaven, Germany.
- Schneider, B., R. Schlitzer, G. Fischer, and E.-M. Nöthig (2003), Depth-dependent elemental compositions of particulate organic matter (POM) in the ocean, *Global Biogeochem. Cycles*, 17(2), 1032, doi:10.1029/2002GB001871.
- Shaffer, G., J. Bendtsen, and O. Ulloa (1999), Fractionation during remineralization of organic matter in the ocean, *Deep Sea Res.*, 46, 185–204.
- Siegenthaler, U., and J. Sarmiento (1993), Atmospheric carbon dioxide and the ocean, *Nature*, 365, 119–125.
- Suess, E. (1980), Particulate organic carbon flux in the ocean: Surface productivity and oxygen utilization, *Nature*, 280, 260–263.
- Toggweiler, J. (1993), Carbon overconsumption, *Nature*, 363, 210–211.
- Volk, T., and M. I. Hoffert (1985), Ocean carbon pumps: Analysis of relative strengths and efficiencies in ocean-driven atmospheric CO<sub>2</sub> changes, in *The Carbon Cycle and Atmospheric CO<sub>2</sub>: Natural Variations Archean to Present*, *Geophys. Monogr. Ser.*, vol. 32, edited by E. Sundquist and W. S. Broecker, pp. 99–110, AGU, Washington D. C.
- Wolf-Gladrow, D., U. Riebesell, S. Burkhardt, and J. Bijma (1999), Direct effects of CO<sub>2</sub> concentration on growth and isotopic composition of marine plankton, *Tellus, Ser. B*, 51, 461–476.
- Wong, C. S., N. A. D. Waser, Y. Nojiri, F. A. Whitney, J. S. Page, and J. Zeng (2002), Seasonal cycles of nutrients and dissolved inorganic carbon at high and mid latitudes in the North Pacific Ocean during the *Skaugran* cruises: Determination of new production and nutrient uptake ratios, *Deep Sea Res.*, 49, 5317–5338.
- Zondervan, I., R. Zeebe, B. Rost, and U. Riebesell (2001), Decreasing marine biogenic calcification: A negative feedback on rising atmospheric pCO<sub>2</sub>, *Global Biogeochem. Cycles*, 15, 507–516.
- Zondervan, I., B. Rost, and U. Riebesell (2002), Effect of CO<sub>2</sub> concentration on the PIC/POC ratio in the coccolithophore *emiliana huxleyi* grown under light-limiting conditions and different daylengths, *J. Exper. Biol. Ecol.*, 272, 55–70.

A. Engel and R. Schlitzer, Alfred Wegener Institut für Polar- und Meeresforschung, PF 120161, D-27515 Bremerhaven, Germany.

B. Schneider, Institut für Geowissenschaften, Ludwig-Meyn-Strasse 10, D-24098 Kiel, Germany. (birgit@passagen.uni-kiel.de)